



## Experimental study of Si–Al substitution in calcium-silicate-hydrate (C–S–H) prepared under equilibrium conditions

Xiaolin Pardal, Isabelle Pochard <sup>\*</sup>, André Nonat

Institut Carnot de Bourgogne, UMR 5209 CNRS-Université de Bourgogne, 9 Av. A. Savary, BP 47 870, F-21078 DIJON Cedex, France

### ARTICLE INFO

#### Article history:

Received 17 June 2008

Accepted 7 May 2009

#### Keywords:

Calcium-silicate-hydrate (C–S–H)

Aluminium

Thermodynamic equilibria

Chemistry

### ABSTRACT

C–A–S–H of varying Al/Si and Ca/(Al + Si) ratios have been prepared introducing C–S–H (Ca/Si = 0.66 and 0.95) at different weight concentrations in a solution coming from the hydration of tricalcium aluminate ( $\text{Ca}_3\text{Al}_2\text{O}_6$ ) in water. XRD and EDX (TEM) analyses show that using this typical synthesise procedure, pure C–A–S–H is obtained only for calcium hydroxide concentrations below  $4.5 \text{ mmol L}^{-1}$ . Otherwise, calcium carboaluminate or strätlingite is also present beside C–A–S–H. The tobermorite-like structure is maintained for C–A–S–H. A kinetic study has shown that the formation of C–A–S–H is a fast reaction, typically less than a few hours. The Ca/(Al + Si) ratio of C–A–S–H matches the Ca/Si ratio of the initial C–S–H, in the ionic concentration range studied i.e., less than 4.5 and 3  $\text{mmol L}^{-1}$  of calcium hydroxide and aluminium hydroxide respectively. The Al/Si ratio increases with the aluminium concentration in the solution and reaches a maximum value of 0.19.

© 2009 Elsevier Ltd. All rights reserved.

### 1. Introduction

When Portland cement is hydrated, the main appearing component is calcium-silicate-hydrate (C–S–H) which results from the silicate phase hydration [1]. The C–S–H nanoparticles are responsible for the cement paste setting through electrostatic forces occurring between them [2–4]. Many studies have been devoted to the study of pure C–S–H from the thermodynamic and structural point of view. Aluminate phases are the second most important constituent of Portland cement, just after silicate phases [5]. It is well-known that aluminium may substitute silicon in C–S–H [6–9]. Therefore, the C–S–H occurring in a cement paste should not be pure C–S–H but Al-substituted-C–S–H named as C–A–S–H.

The numerous studies devoted to the aluminium/silicon substitution in C–S–H allowed to specify the structural aspects of the substitution. For example, Kalousek [10] suggested that aluminium occurs primarily in the tetrahedral sites substituting for silicon whereas Komarneni et al. [11–13] demonstrated that tetrahedral Al occurs in both  $\text{Q}^2$  chain sites and  $\text{Q}^3$  sites that link across interlayer, and significantly affects its cation exchange properties. More recent studies especially using NMR techniques [8,14–19] gave a more detailed description of the Al environment. However, the chemistry of the samples is generally not well-controlled. Either the synthesised C–A–S–H is mixed with other aluminate phases or alkali salts are employed [5,7,14,20–23] which confuses the results, because it is well-known that sodium plays an important role in charge balancing Al[III] for Si[IV] substitution [24]. Until now, there is no determination of the

thermodynamic conditions required for such a substitution, neither its consequences on the cohesion of the resulting C–A–S–H particles. Some questions also remain about a possible location of aluminium in interlayer for example. The present work focuses on the chemical composition of pure C–A–S–H under various equilibrium conditions rather than on the C–A–S–H structure. To do so, pure C–A–S–H of varying stoichiometry among varying equilibrium conditions is needed. Faucon et al. [14] showed that the amount of aluminium present in the C–A–S–H is proportional to the aluminium concentration in the equilibrium solution. Therefore, the idea was to equilibrate C–S–H in solution containing increasing concentration of aluminate ions. In order to avoid the presence of undesired ions such as alkali ions, tricalcium aluminate was hydrated in water and the resulting solution was employed. Doing so, only C–S–H-constituting elements (Ca, Si, O and H) and aluminium were present in the system. In order to vary the amount of aluminium in the solution versus the amount of C–S–H, the liquid ( $\text{Ca}_3\text{Al}_2\text{O}_6$  solution) to solid (C–S–H) ratio was varied. This procedure successfully leads to pure C–A–S–H samples in some conditions. These conditions are not necessarily representative of a Portland cement paste but the main purpose of the present study is to better understand the thermodynamics of C–A–S–H under various conditions allowing the modelling of what occurs in a cement paste.

After describing in details the experimental procedure to synthesise C–A–S–H, the characterization results obtained by solution analyses, XRD and EDX (TEM) will be presented. These results allow determining the equilibrium conditions for the occurrence of pure C–A–S–H and the resulting stoichiometry in terms of Ca/(Al + Si) and Al/Si ratios.

These chemical results will be completed by a structural study conducted by  $^{27}\text{Al}$  and  $^{29}\text{Si}$  MAS NMR and presented in a forthcoming

<sup>\*</sup> Corresponding author.

E-mail address: [isabelle.pochard@u-bourgogne.fr](mailto:isabelle.pochard@u-bourgogne.fr) (I. Pochard).

paper. All these experimental results will be useful to develop a thermodynamic model describing C-A-S-H in equilibrium with electrolytic solutions. The final purpose of this whole work will be to study the consequence on the cohesion of C-S-H particles.

## 2. Experimental

### 2.1. Techniques

The pH measurements were performed with a TACUSSEL MINISIS 8000 pH-meter and a Radiometer Analytical high alkalinity combined pH electrode (Ag/AgCl) XC 250. Standardisation was carried out with buffer solutions at pH 7, 10 and 12.

All the solution analyses (calcium, silicon and aluminium) were done with a VISTA-PRO VARIAN ICP-OES. The standardisation was carried out with own made standards containing calcium, silicon and aluminium (if present in the samples) together in order to re-form the same matrix as in the samples. Each sample was analysed three times, which allows to estimate the error on the concentration to 0.01 mmol L<sup>-1</sup>.

The X-ray Diffraction data were recorded using an Inel CPS 120 position sensitive detector ranging from 8 to 60° 2θ, and a Cu Kα<sub>1</sub> radiation (λ = 1.54056 Å) selected using a quartz slide monochromator. The experimental conditions are: acquisition time = 12 h; voltage = 40 kV; intensity = 40 mA.

The chemical analyses of the solids were carried out using a JEOL JED 2300T Energy Dispersive X-ray Spectrometer (EDX) which is attached to a JEOL 2100 200 kV Transmission Electron Microscope (TEM) fitted with a hairpin type LaB6 filament. The specimen preparation procedure used in this study was the dispersion of the powder in an ethanol solution, the deposition onto a formvar/carbon film supported by a copper grid and the evaporation in air of the drop of the liquid.

### 2.2. Synthesis

The Al-substituted-C-S-H (C-A-S-H) samples were synthesised by a three-step procedure: 1 – synthesis of C-S-H; 2 – preparation of calcium aluminate solution by hydrating tricalcium aluminate (Ca<sub>3</sub>Al<sub>2</sub>O<sub>6</sub>) in diluted suspension; 3 – addition of C-S-H powder in the filtered Ca<sub>3</sub>Al<sub>2</sub>O<sub>6</sub> hydration solution. Several series with different Ca/Si ratios of initial C-S-H and different C-S-H/solution ratios have been prepared. The procedure is described in details below.

#### 2.2.1. Synthesis of C-S-H

C-S-H samples, with Ca/Si molar ratios of 0.66, 0.95 and 1.42 were synthesised from calcium oxide, silica and water according to the quantities listed in Table 1. Calcium oxide was obtained by overnight decarbonation, at 1000 °C, of calcium carbonate provided by Aldrich. Amorphous precipitated silica with a specific area of 230 m<sup>2</sup> g<sup>-1</sup> was provided by Rhodia. Freshly demineralized water was added so as to obtain a water/solid ratio of 50. After one week stirred in a

**Table 1**

Mass of reactants used for the synthesis of C-S-H 0.66, 0.85 and 1.42, and composition of filtrates and solids.

Sample		C-S-H 0.66	C-S-H 0.95	C-S-H 1.42
Mass of reactants (g)	CaO	1.89	2.29	3.00
	SiO <sub>2</sub>	3.09	2.57	2.07
	H <sub>2</sub> O	250	250	250
Filtrates analyses	[Ca] mmol L <sup>-1</sup>	1.48	3.35	16.38
	[Si] mmol L <sup>-1</sup>	3.45	0.08	0.01
	pH	10.05	11.80	12.25
	Water (% w/w)	22.23	18.99	20.70
Solid analyses	Ca/Si from solution	0.66	0.94	1.44
	Ca/Si from solid	0.67	0.97	1.44

See text for details on filtrates and solid analyses.

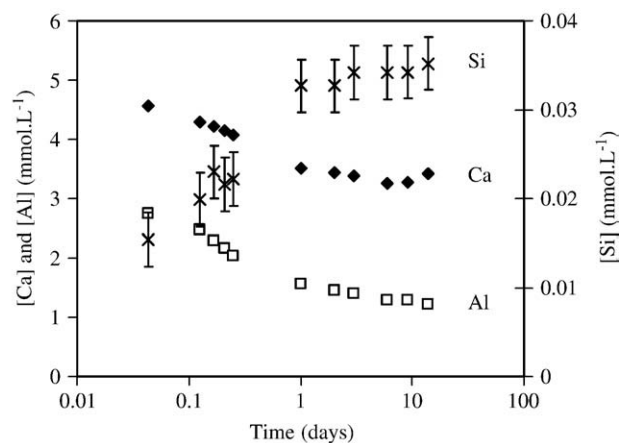


**Fig. 1.** Time evolution of the calcium, aluminium and silicon concentrations in the Ca<sub>3</sub>Al<sub>2</sub>O<sub>6</sub> hydration solution within 10.3 mmol L<sup>-1</sup> of C-S-H 0.66.

thermoregulated bath at 23 °C, the samples were filtered and the composition of the filtrates was determined by ICP-OES analyses and pH measurements (see results in Table 1). Then, the solids were washed two times with an alcohol–water mix, once with pure alcohol, dried in vacuum conditions for 5 days using a membrane pump and finally stored in a desiccator.

The Ca/Si ratios of the C-S-H samples were determined directly on the solids by alkali fusion [25] and also by difference between the added amount of reactants and the remaining calcium and silicon amount in the C-S-H equilibrium solutions. The alkali fusion was performed as follows: 0.2 g of C-S-H and 1 g of LiBO<sub>2</sub> were fused together at 1000 °C for 30 min. The resulting liquid was diluted in 200 mL of 5% hydrochloric acid just after the exit of the furnace, and the calcium and silicon concentrations in this solution were determined by ICP-OES. The overall water content (free and bound water) in the samples was determined by weight loss at 1000 °C during 12 h. All the results are reported in Table 1.

#### 2.2.2. Calcium aluminate solution – Ca<sub>3</sub>Al<sub>2</sub>O<sub>6</sub> hydration

Tricalcium aluminate (Ca<sub>3</sub>Al<sub>2</sub>O<sub>6</sub>, cubic) was hydrated in pure water with a weight ratio of water/Ca<sub>3</sub>Al<sub>2</sub>O<sub>6</sub> = 1000 at 25 °C for 10 days. Then the suspensions were filtered on a MILLIPORE system (0.1 μm), the filtrate was kept carefully to minimize CO<sub>2</sub> contamination and analysed by ICP-OES in order to obtain the concentration of calcium and aluminate ions.

#### 2.2.3. Synthesis of C-A-S-H

Known weights of previously synthesised C-S-H were added in given volumes of fresh Ca<sub>3</sub>Al<sub>2</sub>O<sub>6</sub> filtrate, so as to obtain different C-S-H molar concentrations, C<sub>C-S-H</sub> (mmol L<sup>-1</sup>), ranging from 0.00 to 26.45, 28.30 and 21.53 mmol L<sup>-1</sup> for C-S-H 0.66, 0.95 and 1.42 respectively. C<sub>C-S-H</sub> (mmol L<sup>-1</sup>) is calculated as follows:

$$[C_{\text{C-S-H}}] = \frac{\text{mass dry C-S-H}}{xM_{\text{CaO}} + M_{\text{SiO}_2}} \times \frac{1}{\text{volume of solution}}$$

where  $M_{\text{CaO}}$  and  $M_{\text{SiO}_2}$  are the molar weights (g mol<sup>-1</sup>) of CaO and SiO<sub>2</sub> respectively.

A kinetic study of the ionic composition evolution of the Ca<sub>3</sub>Al<sub>2</sub>O<sub>6</sub> solution among C-S-H addition was performed with C<sub>C-S-H</sub> 0.66 = 10.3 mmol L<sup>-1</sup>. Fig. 1 shows that the ionic composition of the solution changes drastically within the first minutes after the introduction of the C-S-H. After a few hours, the concentrations become constant and they do not change anymore among 14 days. Therefore, the ionic exchanges between the solution and the solid are fast (few minutes) and after one day, the system has reached equilibrium. This equilibrium time of one day

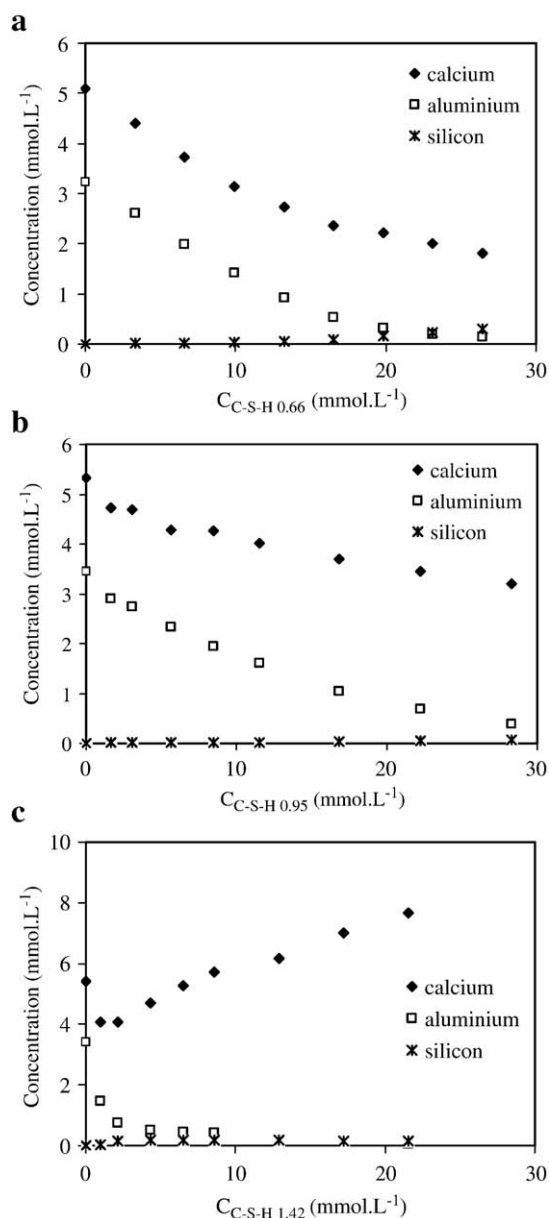


**Fig. 2.** a: Calcium, silicon and aluminium concentrations in  $\text{Ca}_3\text{Al}_2\text{O}_6$  hydration solutions against C-S-H 0.66 added concentration (mmol of C-S-H 0.66 per litre of  $\text{Ca}_3\text{Al}_2\text{O}_6$  solution). b: Calcium, silicon and aluminium concentrations in  $\text{Ca}_3\text{Al}_2\text{O}_6$  hydration solutions against C-S-H 0.95 added concentration (mmol of C-S-H 0.95 per litre of  $\text{Ca}_3\text{Al}_2\text{O}_6$  solution). c: Calcium, silicon and aluminium concentrations in  $\text{Ca}_3\text{Al}_2\text{O}_6$  hydration solutions against C-S-H 1.42 added concentration (mmol of C-S-H 1.42 per litre of  $\text{Ca}_3\text{Al}_2\text{O}_6$  solution).

has been chosen for all the syntheses. After one day of stirring, the suspensions were filtered to separate the liquid and the solid phases. Solids were washed and dried as described in Section 2.2.1 and then analysed by XRD and EDX. Solutions were analysed by ICP-OES.

### 3. Results and discussion

#### 3.1. Evolution of $\text{Ca}_3\text{Al}_2\text{O}_6$ hydration solution throughout C-S-H addition

The initial  $\text{Ca}_3\text{Al}_2\text{O}_6$  filtrate and each sample filtrate were analysed by ICP-OES to measure the calcium, silicon and aluminium concentrations in the equilibrium solutions. Fig. 2-a,b,c presents these concentrations according to the C-S-H added concentration  $C_{\text{C-S-H}}$  (mmol  $\text{L}^{-1}$ ) in the  $\text{Ca}_3\text{Al}_2\text{O}_6$  filtrate for C-S-H 0.66, 0.95 and 1.42 respectively. The points

at  $C_{\text{C-S-H}} = 0$  mmol  $\text{L}^{-1}$  correspond to the pure  $\text{Ca}_3\text{Al}_2\text{O}_6$  filtrate (without added C-S-H).

Fig. 2-a,b,c shows that, due to the C-S-H solubility, the silicon concentration increases very slightly upon C-S-H addition. For the C-S-H 0.66 and 0.95 series, when the amount of C-S-H added is very low, the calcium concentration remains close to the one in the  $\text{Ca}_3\text{Al}_2\text{O}_6$  solution ( $[\text{Ca}^{2+}] \approx 5.2$  mmol  $\text{L}^{-1}$ ), whereas when the C-S-H molar concentration is increased, the calcium concentration tends toward the C-S-H solubility: for  $C_{\text{C-S-H}} > 20$  mmol  $\text{L}^{-1}$ ,  $[\text{Ca}^{2+}]$  rises 1.80 and 3.21 mmol  $\text{L}^{-1}$  in Fig. 2-a and b respectively. These two values are close to the calcium concentrations listed in Table 1 for the equilibrium solution of C-S-H 0.66 ( $[\text{Ca}^{2+}] = 1.48$  mmol  $\text{L}^{-1}$ ) and C-S-H 0.95 ( $[\text{Ca}^{2+}] = 3.35$  mmol  $\text{L}^{-1}$ ).

The behaviour is different for the C-S-H 1.42 series where the composition of the solution does not reach the solubility of C-S-H 1.42

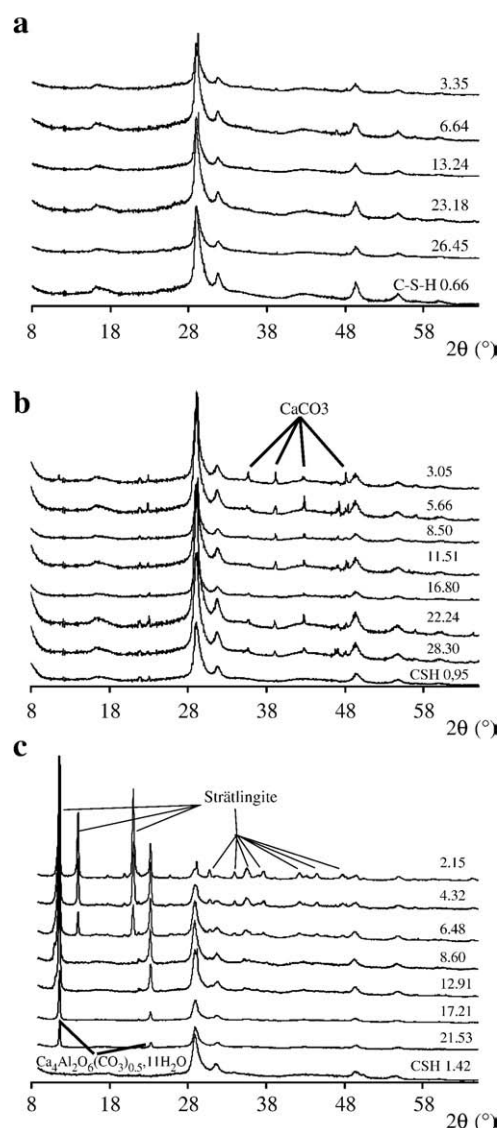


**Fig. 3.** a: XRD patterns of the powdered samples obtained from mixing C-S-H 0.66 in  $\text{Ca}_3\text{Al}_2\text{O}_6$  hydration solution. The initial C-S-H 0.66 pattern is also shown for comparison. The number on each curve corresponds to the C-S-H concentration,  $C_{\text{C-S-H}}$ , in mmol  $\text{L}^{-1}$  in the  $\text{Ca}_3\text{Al}_2\text{O}_6$  hydration solution. b: XRD patterns of the powdered samples obtained from mixing C-S-H 0.95 in  $\text{Ca}_3\text{Al}_2\text{O}_6$  hydration solution. The initial C-S-H 0.95 pattern is also shown for comparison. The number on each curve corresponds to the C-S-H concentration,  $C_{\text{C-S-H}}$ , in mmol  $\text{L}^{-1}$  in the  $\text{Ca}_3\text{Al}_2\text{O}_6$  hydration solution. c: XRD patterns of the powdered samples obtained from mixing C-S-H 1.42 in  $\text{Ca}_3\text{Al}_2\text{O}_6$  hydration solution. The initial C-S-H 1.42 pattern is also shown for comparison. The number on each curve corresponds to the C-S-H concentration,  $C_{\text{C-S-H}}$ , in mmol  $\text{L}^{-1}$  in the  $\text{Ca}_3\text{Al}_2\text{O}_6$  hydration solution.

which is  $16.38 \text{ mmol L}^{-1}$  according to Table 1. Actually, the calcium hydroxide concentration in the initial  $\text{Ca}_3\text{Al}_2\text{O}_6$  solution equals  $5.5 \text{ mmol L}^{-1}$ . According to the C-S-H stoichiometry (in terms of Ca/Si ratio) versus calcium hydroxide concentration in the equilibrium solution [26–32], the  $\text{Ca}_3\text{Al}_2\text{O}_6$  solution is not able to fix a high Ca/Si ratio, close to the one in saturated calcium hydroxide solution. Furthermore, the variations of the calcium concentration in this series are not similar to the 0.66 and 0.95 series. One can notice that it decreases among the first addition of C-S-H 1.42 and then increases with more C-S-H 1.42 added.

The variations of aluminium concentration are also different for series 1.42 compared to the two others. The noteworthy relationship between the added amount of C-S-H 0.66 and 0.95 and the decrease in the aluminium concentration is a good hint that aluminates incorporate the C-S-H. It seems not to be the case for C-S-H 1.42 for which the aluminium concentration falls down rapidly below  $1 \text{ mM}$  for  $\text{C-S-H}_{1.42} > 2.15 \text{ mmol L}^{-1}$  and then tends toward zero for further addition of C-S-H 1.42.

### 3.2. Characterization of the solid samples

#### 3.2.1. XRD analyses

All the solids have been analysed by XRD except the samples of  $\text{C-S-H}_{0.95} = 1.62 \text{ mmol L}^{-1}$  and  $\text{C-S-H}_{1.42} = 0.96 \text{ mmol L}^{-1}$  because the mass of sample available was not sufficient to carry out a powder diffraction analysis.

All the XRD patterns in Fig. 3-a,b,c show typical tobermorite-type C-S-H. For the C-S-H 0.66 series, only one pure C-S-H-like phase is detected. No additional phases, like strätlingite or AFm were detected, which is not the case in other studies [12,22]. The same observation is found for the C-S-H 0.95 series, except that calcite is detected in all these samples. Nevertheless, the carbonation is limited and the slight amount of calcite present would have no significant effect on the C-A-S-H formation. Carbonation only results in the consumption of  $\text{OH}^-$  and decreases the pH. The very weak amount of calcium carbonate which is observed comparatively to the high volume of solution has a very small incidence on the pH of the solution.

These results demonstrate that the drop of aluminium concentration observed in Fig. 2-a and b is due to the insertion of aluminate ions in the C-S-H, leading to the formation of C-A-S-H. In the  $2\theta$  range studied, no modification of the C-S-H pattern is observed. This means that the Al insertion in C-S-H induces no strong structural changes in the solid. Sun et al. [22] have reported that the basal spacing (derived from the (002) peak) increases significantly with increasing Al content in the C-S-H. The low-angle reflections have not been evaluated in the present study. Therefore we cannot state on this point.

For the C-S-H 1.42 series, Fig. 3-c exhibits that AFm phases, calcium carboaluminate ( $\text{Ca}_4\text{Al}_2\text{O}_6(\text{CO}_3)_{0.5} \cdot 11\text{H}_2\text{O}$ ) and strätlingite ( $\text{Ca}_2\text{Al}_2\text{SiO}_7 \cdot 8\text{H}_2\text{O}$ ) are observed beside the C-S-H phase. In these series, due to the increase of the pH, the concentration of carbonate in solution increases also. By this way, the solution becomes supersaturated with respect to hemi- and perhaps monocarboaluminate which precipitate. The occurrence of AFm phases beside C-S-H in this series is in agreement with the results in Fig. 2-c where it has been observed that C-S-H 1.42 behaves in a different way in  $\text{Ca}_3\text{Al}_2\text{O}_6$  hydration solution than C-S-H 0.66 and 0.95.

As a consequence, the aluminate concentration corresponding to the solubility of these carboaluminate phases is much lower than the one corresponding to hydroxyl AFm phase (respectively 0.1, 0.05 and  $2 \text{ mM}$  in  $10 \text{ mM}$  calcium hydroxide solution (calculated after [33–35]) as seen in Fig. 2-c).

#### 3.2.2. Elemental analyses (EDX, TEM)

The XRD analyses reported above indicate that C-A-S-H free of crystalline aluminate phase is obtained from the C-S-H 0.66 and 0.95 series. However, one can wonder if amorphous aluminate like aluminium hydroxide could be present in these samples. Therefore, the elemental

composition of a Al-rich sample (synthesised from  $13.24 \text{ mmol L}^{-1}$  of C-S-H 0.66) was extracted from the EDX chemical analyses by TEM. Especially, the homogeneity of the sample has been verified. Unfortunately, C-S-H like all hydrates is unstable under vacuum conditions and the analyses should not exceed 2 h, which corresponds to about 15–20 analyses per sample. Three samples (synthesised from  $13.24 \text{ mmol L}^{-1}$  of C-S-H 0.66) have been probed. The elemental analyses in terms of Ca/(Al + Si) and Al/Si ratios are depicted in Fig. 4-a and b.

The results show that the Ca/(Al + Si) distribution is quite narrow and centred to  $0.6 \pm 0.1$  and the Al/Si ratio values are centred to 0.20–0.25. This indicates that the sample is chemically homogeneous and that no Al-rich phase exists. Therefore, the occurrence of an Al amorphous gel within the C-A-S-H does not seem to occur.

According to Fig. 2-a, the C-A-S-H obtained from  $\text{C-S-H}_{0.66} = 13.24 \text{ mmol L}^{-1}$  is in equilibrium with a solution containing  $2 \text{ mmol L}^{-1}$  of calcium hydroxide. This is about the same equilibrium concentration as C-S-H 0.66 suspensions [26–32]. It means that C-S-H 0.66 and this C-A-S-H sample get the same calcium content. Moreover, Fig. 4-a indicates a Ca/(Al + Si) ratio very close to 0.66 for this C-A-S-H. Therefore, the C-S-H 0.66 Si content and the C-A-S-H (Al + Si) content have to be very close in order to get the same Ca/Si and Ca/(Al + Si) ratios. This means that, for this low Ca/Si ratio, the main part of the aluminate ions inserted in the solid is not in addition to the silicate ions but a substitute part of the latter. This is in agreement with other studies showing that aluminate ions substitute bridging silicate according to a tobermorite-like structure [12,14,22,24]. These studies

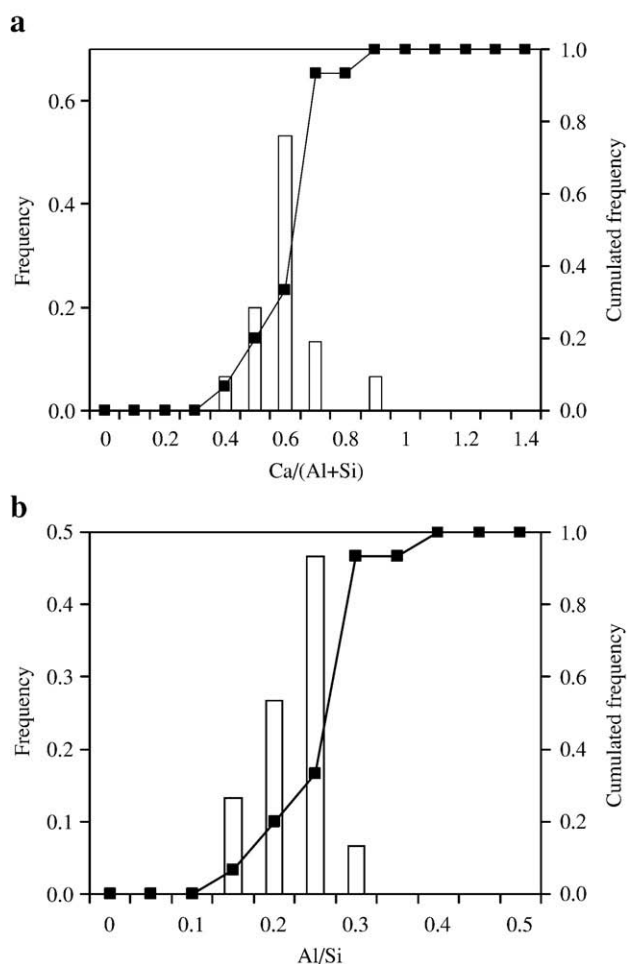
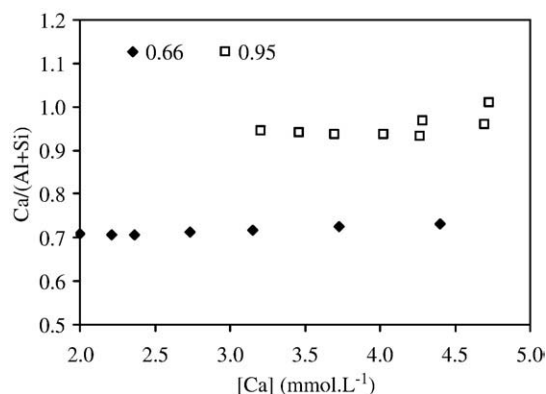


Fig. 4. a: Elemental analyses (EDX, TEM) expressed in Ca/(Al + Si) ratio for the solid obtained from  $\text{C-S-H}_{0.66} = 13.24 \text{ mmol L}^{-1}$ . b: Elemental analyses (EDX, TEM) expressed in Al/Si ratio for the solid obtained from  $\text{C-S-H}_{0.66} = 13.24 \text{ mmol L}^{-1}$ .





**Fig. 5.** Evolution of the  $\text{Ca}/(\text{Si} + \text{Al})$  ratio of C-A-S-H synthesised from C-S-H 0.66 and 0.95 versus calcium hydroxide concentration in the equilibrium solution. The  $\text{Ca}/(\text{Si} + \text{Al})$  ratio values are calculated from mass conservation and chemical analyses of solids and solutions.

indicate an Al/Si ratio close to 1/6 which is in good agreement with the present value obtained by EDX.

Whereas the  $\text{Ca}/(\text{Al} + \text{Si})$  distributions are narrow and in very good agreement with the  $\text{Ca}/\text{Si}$  ratio of the initial C-S-H employed ( $\text{Ca}/\text{Si} = 0.66$ ), the Al/Si distributions are somewhat dispersed. Actually, this comes from the very low quantity of Al, no more than a few atomic percent, in the sample which implies a significant inaccuracy in the EDX analyses. Therefore, a more accurate chemical analysis is needed to get the stoichiometry of all the samples. This has been done by the difference between the initial and equilibrium concentrations in solution and is presented in Section 3.3.

### 3.3. Stoichiometry of C-A-S-H

The stoichiometry of each solid, in terms of Al/Si and  $\text{Ca}/(\text{Al} + \text{Si})$ , has been determined by subtracting the quantities of Al, Ca and Si present in the equilibrium solution (determined by ICP-OES) to the initial amounts of Al, Ca and Si coming from the  $\text{Ca}_3\text{Al}_2\text{O}_6$  hydration solution and the C-S-H added. The  $\text{Ca}/(\text{Si} + \text{Al})$  versus calcium hydroxide concentration and the Al/Si ratios versus the aluminium bulk concentration for the C-A-S-H synthesised from C-S-H 0.66 and 0.95 are reported in Figs. 5 and 6 respectively. The result for C-A-S-H synthesised from C-S-H 1.42 is not reported as it does not really make sense because of the presence of several phases.

#### 3.3.1. $\text{Ca}/(\text{Al} + \text{Si})$ ratio

For C-S-H, it is well-known that the  $\text{Ca}/\text{Si}$  ratio increases with the calcium hydroxide concentration of the equilibrium solution. This is

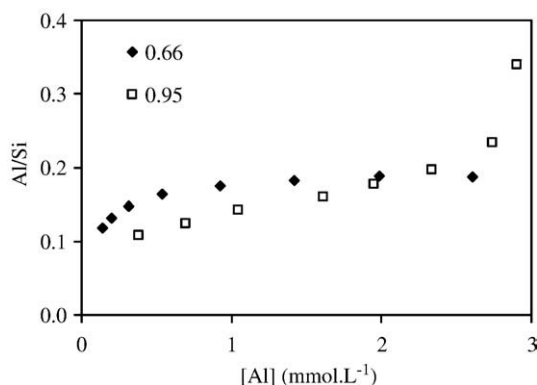


**Fig. 6.** Evolution of the Al/Si ratio of the solid fraction of the three series of C-A-S-H from C-S-H 0.66 and 0.95, versus aluminate concentration in the equilibrium solution. The Al/Si ratio values are calculated from mass conservation and chemical analyses of solids and solutions.

due to an increase of the C-S-H calcium content and a decrease of the silicon one. These two features should also occur for C-A-S-H. However, Fig. 5 shows that for the C-A-S-H synthesised from C-S-H 0.66 and 0.95, no change in the  $\text{Ca}/(\text{Si} + \text{Al})$  ratio occurs against the calcium hydroxide bulk concentration. It remains at  $0.70 \pm 0.05$  and  $0.95 \pm 0.05$  respectively. Therefore, in order to maintain the  $\text{Ca}/(\text{Al} + \text{Si})$  ratio constant, the aluminium amount in the solid has to compensate first the silicon loss by Al/Si substitution, and second the calcium gain. This is in agreement with recent structural studies [5,6,22] showing that aluminium is mainly in substitution of silicon but also, some are in insertion at the surface or in the interlayer of the C-A-S-H particles. According to these studies, these extra aluminium ions balance the excess negative charge created by the  $\text{Al}^{3+}/\text{Si}^{4+}$  substitution.

#### 3.3.2. Al/Si ratio

For C-A-S-H synthesised from C-S-H 0.66, Al/Si aims towards a quasi-constant plateau, which would mean that the Al saturation of C-A-S-H has been reached. The maximum Al/Si ratio in the C-A-S-H is 0.19, which is in agreement with several studies in the literature [12,14,22,24], reporting that approximately 1/6 of all tetrahedra, or 1/2 of the bridging tetrahedra, for a fully polymerized structure, were substituted. The present results are in agreement with the lower limit of the EDX analyses of Section 3.2.2. The slight discrepancy with the EDX results comes from the very low quantity of Al, no more than a few atomic percent, in the sample which implies a significant inaccuracy in the EDX analyses.

For the lower aluminium concentrations, the Al/Si ratio of C-A-S-H synthesised from C-S-H 0.95 is significantly lower than the Al/Si ratio of C-A-S-H synthesised from C-S-H 0.66. Indeed, Fig. 6 shows that for  $[\text{Al}] < 1 \text{ mmol L}^{-1}$ , Al/Si for C-A-S-H prepared from C-S-H 0.66 rises 0.18 whereas Al/Si for C-A-S-H prepared from C-S-H 0.95 is no more than 0.13. In fact, the difference between both series is the calcium hydroxide concentration. The latter is greater in the 0.95 series ( $3\text{--}4 \text{ mmol L}^{-1}$  for 0.95 series and  $2 \text{ mmol L}^{-1}$  for 0.66 series according to Fig. 2-a and b). Then, when the aluminium concentration is increased up to  $2 \text{ mmol L}^{-1}$ , the calcium hydroxide concentration for both series becomes the same (around  $4 \text{ mmol L}^{-1}$  according to Fig. 2-a and b). Consequently, the Al/Si ratio for both series becomes the same too. Therefore, the Al/Si ratio is constant for a given solution composition i.e., same aluminium and calcium hydroxides concentrations. It means that C-A-S-H is in equilibrium within its interstitial solution. Finally, the Al/Si ratio of C-A-S-H from C-S-H 0.95 starts to increase exponentially for the last sample at  $[\text{Al}] = 2.9 \text{ mM}$  ( $\text{Al/Si} = 0.34$ ). This would mean that for this latter sample, for which no XRD analyses had been possible because solid was not sufficient, AFm phases precipitate beside C-A-S-H.

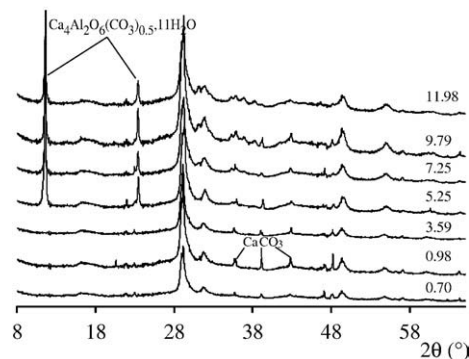


**Fig. 7.** XRD patterns of C-A-S-H ( $\text{Al/Si} = 0.19$ ,  $\text{Ca}/(\text{Si} + \text{Al}) = 0.7$ ) equilibrated in different calcium hydroxide solutions. The weight concentration of C-A-S-H in the calcium hydroxide solutions is  $2 \text{ g L}^{-1}$ . The equilibrium calcium hydroxide concentrations are depicted on the graph.

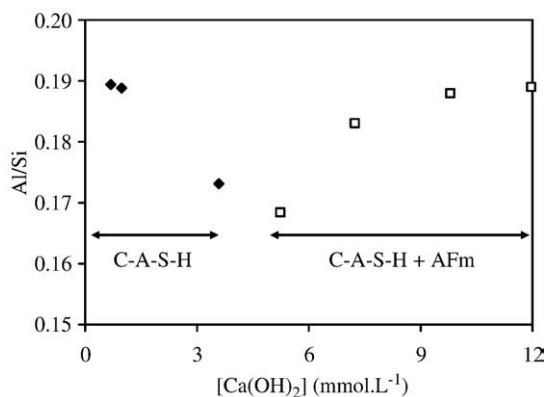


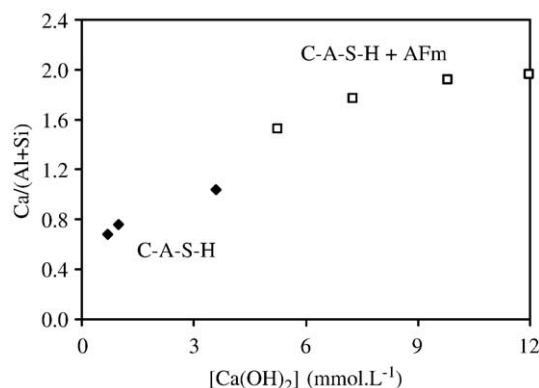
**Fig. 8.** Evolution of the Al/Si ratio of the solid against the calcium hydroxide concentration when initial C-A-S-H ( $\text{Al/Si} = 0.19$ ,  $\text{Ca}/(\text{Si} + \text{Al}) = 0.7$ ) is equilibrated in calcium hydroxide solutions of increasing concentrations. The filled diamonds and the open squares correspond to pure C-A-S-H and a blending of C-A-S-H and calcium carboaluminate respectively.

### 3.4. C-A-S-H in calcium hydroxide solutions

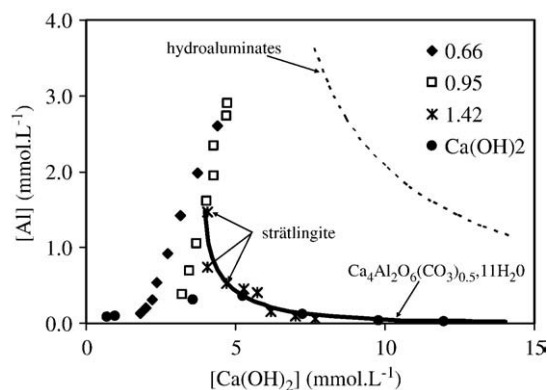
So far, the conclusion is that no pure C-A-S-H of  $\text{Ca}/(\text{Al} + \text{Si}) > 0.95$  can be prepared by immersing C-S-H in  $\text{Ca}_3\text{Al}_2\text{O}_6$  hydration solution. It is disappointing as the high calcium hydroxide concentration occurring in a typical cement paste stresses high  $\text{Ca}/(\text{Al} + \text{Si})$  ratios. Another way to succeed in preparing C-A-S-H of high  $\text{Ca}/(\text{Al} + \text{Si})$  is maybe to equilibrate pure C-A-S-H of low  $\text{Ca}/(\text{Al} + \text{Si})$  in calcium hydroxide solutions of increasing concentrations. To do so, previously synthesised C-A-S-H ( $\text{Al/Si} = 0.19$ ,  $\text{Ca}/(\text{Si} + \text{Al}) = 0.7$ ) was immersed at a weight concentration of  $2 \text{ g L}^{-1}$  in calcium hydroxide solutions. The initial calcium hydroxide concentrations were  $0 \text{ mmol L}^{-1}$ ,  $0.84 \text{ mmol L}^{-1}$ ,  $5.5 \text{ mmol L}^{-1}$ ,  $10.9 \text{ mmol L}^{-1}$ ,  $15.2 \text{ mmol L}^{-1}$ ,  $19.1 \text{ mmol L}^{-1}$  and  $21.6 \text{ mmol L}^{-1}$ .

Fig. 7 shows the XRD analyses results of this sample series and the equilibrium calcium hydroxide concentration for each sample. In Fig. 7, one can see that a hydroaluminate calcium carbonate phase is detected in addition to the C-A-S-H phase as soon as the equilibrium calcium hydroxide concentration equals  $5.25 \text{ mmol L}^{-1}$ .

Fig. 8 presents the evolution of the Al/Si ratio for this series against the calcium hydroxide concentration. The occurrence of the calcium carboaluminate for  $[\text{Ca}(\text{OH})_2] \geq 5.25 \text{ mM}$  is well demonstrated in this figure. Actually, below  $5.25 \text{ mM}$ , the Al/Si ratio decreases and the aluminium concentration increases because of the release of aluminate from the C-A-S-H. From  $5.25 \text{ mM}$ , the calcium carboaluminate precipitates as demonstrated by XRD, and consequently, the aluminium concentration starts to decrease and the Al/Si ratio is enhanced.



**Fig. 9.** Evolution of the  $\text{Ca}/(\text{Al} + \text{Si})$  ratio of the solid against the calcium hydroxide concentration when C-A-S-H ( $\text{Al/Si} = 0.19$ ,  $\text{Ca}/(\text{Si} + \text{Al}) = 0.7$ ) is equilibrated in calcium hydroxide solutions of increasing concentrations. Filled diamonds: pure C-A-S-H; open squares: C-A-S-H + AFm.



**Fig. 10.** Aluminium versus calcium concentrations for all the samples studied. The three samples of series “1.42” for which strätlingite has been observed by XRD are pointed out. The solubility curves of  $\text{C}_2\text{AH}_8$  and  $\text{Ca}_4\text{Al}_2\text{O}_6(\text{CO}_3)_{0.5} \cdot 11\text{H}_2\text{O}$  are depicted (dashed and solid curves respectively).

Obviously, this is an overall Al/Si ratio which includes the Al/Si ratios of both the C-A-S-H and the calcium carboaluminate phases.

Fig. 9 shows the evolution of the overall  $\text{Ca}/(\text{Al} + \text{Si})$  ratio of these samples against the calcium hydroxide concentration. In this figure, one can see that the maximum  $\text{Ca}/(\text{Al} + \text{Si})$  ratio of pure C-A-S-H (before carbonate AFm precipitation) equals 1.

Therefore, neither by starting from C-S-H and  $\text{Ca}_3\text{Al}_2\text{O}_6$  hydration solution nor by equilibrating C-A-S-H in calcium hydroxide solutions, it has been possible to synthesise pure C-A-S-H of  $\text{Ca}/(\text{Al} + \text{Si}) > 1$ . In all cases, calcium hydroaluminate phases have been observed.

The aluminium versus calcium concentrations have been plotted for all the studied series (see Fig. 10). The occurrence of pure C-A-S-H can be well-observed in Fig. 10 by comparing these data to the solubility curves of AFm phases. For instance, the presence of calcium hemicarboaluminate for  $[\text{Ca}(\text{OH})_2] \geq 5 \text{ mM}$  observed by XRD analyses is in good agreement with the superimposition of these points with the solubility curve of calcium hemicarboaluminate in Fig. 10.

Without carbon dioxide in the system, perhaps pure C-A-S-H would have been obtained for larger ranges of lime and aluminate concentrations because calcium hydroaluminates are more soluble than calcium carboaluminates as demonstrated by Fig. 10. However, strätlingite has also been observed in a few samples much below the solubility curve of hydroaluminates and with a solubility comparable to  $\text{Ca}_4\text{Al}_2\text{O}_6(\text{CO}_3)_{0.5} \cdot 11\text{H}_2\text{O}$ . Unfortunately, reliable thermodynamic data on the solubility of strätlingite are not available and the presence of strätlingite under various conditions could not be verified. Therefore, the present experimental data could be an interesting starting point to calculate thermodynamic constant concerning strätlingite.

## 4. Conclusion

Al-substituted C-S-H (C-A-S-H) samples were synthesised by a three-step original procedure. This synthesis consists in equilibrating well-defined C-S-H, previously obtained from  $\text{CaO}$ ,  $\text{H}_2\text{O}$  and  $\text{SiO}_2$ , in the hydration solution of tricalcium aluminate ( $\text{Ca}_3\text{Al}_2\text{O}_6$ ). The latter is the filtrate of a  $\text{Ca}_3\text{Al}_2\text{O}_6$  aqueous suspension. This procedure avoids the presence of foreign ions such as alkali. Afterwards, well-defined quantities of C-S-H were added in given volumes of freshly  $\text{Ca}_3\text{Al}_2\text{O}_6$  filtrate, so as to obtain different C-S-H molar concentrations  $C_{\text{C-S-H}}$  ( $\text{mol L}^{-1}$ ). This allows getting C-A-S-H of various Al/Si ratios up to 0.19. A kinetic study showed that the Al insertion in C-S-H is a fast reaction, typically less than one day. The characterization of the solid samples by XRD and EDX (TEM) indicates that pure C-A-S-H is obtained only if the  $\text{Ca}/\text{Si}$  ratio of the initial C-S-H is below 1, which corresponds to a calcium hydroxide concentration below  $4 \text{ mmol L}^{-1}$ . Otherwise, calcium carboaluminate or/and strätlingite are also present beside C-A-S-H. This feature is also observed when pure C-A-S-H,

previously synthesised by the procedure described in the present paper, is equilibrated in calcium hydroxide solutions.

The present experimental data would be of interest for modelling the thermodynamic equilibria in the C-S-H/aluminates system and determine thermodynamic constants. However, the presence of aluminate phases in some samples restricts the knowledge of the C-A-S-H stoichiometry. In these cases, the overall Al/Si ratio includes the Al/Si ratios of both the C-A-S-H and the aluminate phases. In order to get the Al/Si ratio of C-A-S-H alone, semi-quantitative solid-state  $^{27}\text{Al}$  and  $^{29}\text{Si}$  NMR analyses would be of great interest.

## References

- [1] H.F.W. Taylor, *Cement Chemistry*, A. Press, London, 1990.
- [2] A. Nonat, The structure and stoichiometry of C-S-H, *Cement and Concrete Research* 34 (9) (2004) 1521–1528.
- [3] C. Plassard, E. Lesniewska, I. Pochard, A. Nonat, Investigation of the surface structure and elastic properties of calcium silicate hydrates at the nanoscale, *Ultramicroscopy* 100 (3–4) (2004) 331–338.
- [4] C. Plassard, E. Lesniewska, I. Pochard, A. Nonat, Nanoscale experimental investigation of particle interactions at the origin of the cohesion of cement, *Langmuir* 21 (16) (2005) 7263–7270.
- [5] M.D. Andersen, H.J. Jakobsen, J. Skibsted, A new aluminium-hydrate species in hydrated Portland cements characterized by  $^{27}\text{Al}$  and  $^{29}\text{Si}$  MAS NMR spectroscopy, *Cement and Concrete Research* 36 (1) (2006) 3–17.
- [6] M.D. Andersen, H.J. Jakobsen, J. Skibsted, Incorporation of aluminum in the calcium silicate hydrate (C-S-H) of hydrated Portland cements: a high-field  $^{27}\text{Al}$  and  $^{29}\text{Si}$  MAS NMR investigation, *Inorganic Chemistry* 42 (7) (2003) 2280–2287.
- [7] M.D. Andersen, H.J. Jakobsen, J. Skibsted, Characterization of white Portland cement hydration and the C-S-H structure in the presence of sodium aluminate by  $^{27}\text{Al}$  and  $^{29}\text{Si}$  MAS NMR spectroscopy, *Cement and Concrete Research* 34 (5) (2004) 857–868.
- [8] P. Faucon, T. Charpentier, D. Bertrand, A. Nonat, J. Virlet, J.C. Petit, Characterization of calcium aluminate hydrates and related hydrates of cement pastes by  $^{27}\text{Al}$  MQ-MAS NMR, *Inorganic Chemistry* 37 (15) (1998) 3726–3733.
- [9] J.J. Thomas, D. Rothstein, H.M. Jennings, B.J. Christensen, Effect of hydration temperature on the solubility behavior of Ca-, S-, Al-, and Si-bearing solid phases in Portland cement pastes, *Cement and Concrete Research* 33 (12) (2003) 2037–2047.
- [10] G.L. Kalousek, Crystal chemistry of hydrous calcium silicates: I. Substitution of aluminum in lattice of tobermorite, *Journal of the American Ceramic Society* 40 (3) (1957) 74–80.
- [11] S. Komarneni, D.M. Roy, C.A. Fyfe, G.J. Kennedy, Naturally occurring 1.4 nm tobermorite and synthetic jennite: characterisation by  $^{27}\text{Al}$  and  $^{29}\text{Si}$  MAS NMR spectroscopy and cation exchange properties, *Cement and Concrete Research* 17 (6) (1987) 891–895.
- [12] S. Komarneni, R. Roy, D.M. Roy, C.A. Fyfe, G.J. Kennedy, A.A. Bothner-By, J. Dadok, A.S. Chesnick,  $^{27}\text{Al}$  and  $^{29}\text{Si}$  magic angle spinning nuclear magnetic resonance spectroscopy of Al-substituted tobermorites, *Journal of Materials Science* 20 (11) (1985) 4209–4214.
- [13] S. Komarneni, M. Tsuji, Selective cation exchange in substituted tobermorites, *Journal of the American Ceramic Society* 72 (9) (1989) 1668–1674.
- [14] P. Faucon, T. Charpentier, A. Nonat, J.C. Petit, Triple-quantum two-dimensional  $^{27}\text{Al}$  magic angle nuclear magnetic resonance study of the aluminum incorporation in calcium silicate hydrates, *Journal of the American Chemical Society* 120 (46) (1998) 12075–12082.
- [15] P. Faucon, A. Delagrè, J.C. Petit, C. Richet, J.M. Marchand, H. Zanni, Aluminum incorporation in calcium silicate hydrates (C-S-H) depending on their Ca/Si ratio, *Journal of Physical Chemistry B* 103 (37) (1999) 7796–7802.
- [16] I.G. Richardson, The nature of C-S-H in hardened cements, *Cement and Concrete Research* 29 (8) (1999) 1131–1147.
- [17] I.G. Richardson, A.R. Brough, R. Brydson, G.W. Groves, C.M. Dobson, Location of aluminum in substituted calcium silicate hydrate (C-S-H) gels as determined by  $^{29}\text{Si}$  and  $^{27}\text{Al}$  NMR and EELS, *Journal of the American Ceramic Society* 76 (9) (1993) 2285–2288.
- [18] I.G. Richardson, G.W. Groves, A reply to discussions by H.F.W. Taylor of the papers “Models for the composition and structure of calcium silicate hydrate (C-S-H) gel in hardened tricalcium silicate pastes” and “the incorporation of minor and trace elements into calcium silicate hydrate (C-S-H) gel in hardened cement pastes” \*1, \*2, *Cement and Concrete Research* 23 (4) (1993) 999–1000.
- [19] J. Schneider, M.A. Cincotto, H. Panepucci,  $^{29}\text{Si}$  and  $^{27}\text{Al}$  high-resolution NMR characterization of calcium silicate hydrate phases in activated blast-furnace slag pastes, *Cement and Concrete Research* 31 (7) (2001) 993–1001.
- [20] L. Black, A. Stumm, K. Garbev, P. Stemmermann, K.R. Hallam, G.C. Allen, X-ray photoelectron spectroscopy of aluminium-substituted tobermorite, *Cement and Concrete Research* 35 (1) (2005) 51–55.
- [21] S.Y. Hong, F.P. Glasser, Alkali sorption by C-S-H and C-A-S-H gels: part II. Role of alumina, *Cement and Concrete Research* 32 (7) (2002) 1101–1111.
- [22] G.K. Sun, J.F. Young, R.J. Kirkpatrick, The role of Al in C-S-H: NMR, XRD, and compositional results for precipitated samples, *Cement and Concrete Research* 36 (1) (2006) 18–29.
- [23] S.D. Wang, K.L. Scrivener,  $^{29}\text{Si}$  and  $^{27}\text{Al}$  NMR study of alkali-activated slag, *Cement and Concrete Research* 33 (5) (2003) 769–774.
- [24] I. Lognot, I. Klur, A. Nonat, in: P. Colombet, H. Zanni, A. Grimmer, P. Sozzani (Eds.), *Nuclear Magnetic Resonance Spectroscopy of Cement-based Materials*, Springer, Berlin, 1998, pp. 189–196.
- [25] J.C. Farinas, P. Ortega, Chemical analysis of Portland cement by inductively-coupled plasma atomic emission spectrometry, *Analysis* 120 (1992) 221–228.
- [26] X. Cong, R.J. Kirkpatrick,  $^{29}\text{Si}$  MAS NMR study of the structure of calcium silicate hydrate, *Advanced Cement Based Materials* 3 (3–4) (1996) 144–156.
- [27] E.P. Flint, L.S. Wells, Study of the system  $\text{CaO-SiO}_2\text{-H}_2\text{O}$  at 30 °C and of the reaction of water on the anhydrous calcium silicates, *Bureau of Standard Journal of Research* 12 (1934) 751–783.
- [28] S.A. Greenberg, T.N. Chang, Investigation of the colloidal hydrated calcium silicates. II. Solubility relationships in the calcium oxide-silica-water system at 25 °C, *The Journal of Physical Chemistry* 69 (1) (1965) 182–188.
- [29] M.W. Grutzeck, A. Benesi, B. Fanning,  $^{29}\text{Si}$  magic angle spinning nuclear magnetic resonance study of tricalcium silicate hydrate, *Journal of the American Ceramic Society* 72 (4) (1989) 665–668.
- [30] X. Lecoq, Etude de l'hydratation à concentration contrôlée du silicate tricalcique  $\text{Ca}_3\text{SiO}_5$  et des caractéristiques de ses produits de réaction, PhD thesis, University of Bourgogne, Dijon, 1993.
- [31] P.S. Roller, G. Erwin, The system calcium oxide silica water at 30 °C – the association of silicate ion in dilute alkaline solution, *Journal of the American Chemical Society* 62 (1940) 461–471.
- [32] H.F.W. Taylor, Hydrated calcium silicates. Part 1. Compound formation at ordinary temperatures, *Journal of Chemical Society* (1950) 3682–3690.
- [33] D. Damidot, F.P. Glasser, Investigation of the  $\text{CaO-Al}_2\text{O}_3\text{-SiO}_2\text{-H}_2\text{O}$  system at 25 °C by thermodynamic calculations, *Cement and Concrete Research* 25 (1) (1995) 22–28.
- [34] D. Damidot, S. Stronach, A. Kindness, M. Atkins, F.P. Glasser, Thermodynamic investigation of the  $\text{CaO-Al}_2\text{O}_3\text{-CaCO}_3\text{-H}_2\text{O}$  system at 25 °C and the influence of  $\text{Na}_2\text{O}$ , *Cement and Concrete Research* 24 (3) (1994) 563–572.
- [35] S.A. Stronach, F.P. Glasser, Modelling the impact of abundant geochemical components on phase stability and solubility of the  $\text{CaO-SiO}_2\text{-H}_2\text{O}$  system at 25 °C:  $\text{Na}^+$ ,  $\text{K}^+$ ,  $\text{SO}_4^{2-}$ ,  $\text{Cl}^-$  and  $\text{CO}_3^{2-}$ , *Advances in Cement Research* 9 (36) (1997) 167–181.